# SHORT REVIEW ON THERMAL CONDUCTIVITY OF SILICON NITRIDE CERAMICS

by

***Aleksandra B. ŠAPONJIĆ***[a*], ***Sladjana LJ. MASLOVARA***[b], ***and Milan V. GORDIĆ***[a]

[a]Vinča Institute of Nuclear Sciences, National Institute of the Republic of Serbia,
University of Belgrade, Belgrade, Serbia
[b]Institute of General and Physical Chemistry, Belgrade, Serbia

Review paper
https://doi.org/10.2298/TSCI240615187S

*Silicon nitride ($Si_3N_4$) with high thermal conductivity is one of the most promising substrate materials for the next-generation power devices. There are several ways to improve thermal conductivity of $Si_3N_4$. Substantially higher thermal conductivities for the $Si_3N_4$ ceramics could be attained by reduction of lattice oxygen content or by the increasing the $\beta/\alpha$ phase ratio during nitridation thus enhancing grain growth during post-sintering. The method of purification of the grains and decreasing the two-grain junction films by adding large $\beta$-$Si_3N_4$ grains to the raw $Si_3N_4$ powder, seeding by grain growth of $Si_3N_4$ crystals in polycrystalline ceramics also improves thermal conductivity. High thermal conductivity can be further achieved by development a textured micro-structure in which elongated $\beta$-$Si_3N_4$ grains are oriented almost unidirectional. This paper summarizes the extrinsic factors governing the thermal conductivity of $Si_3N_4$ ceramic regarding micro-structural parameters such as lattice defects in single-crystal, sintering additives, change in microstructural parameters like $\alpha/\beta$ ratio, grain size, aspect ratio, grain orientation and the morphology, composition of grain-boundary, secondary phases, processing method.*

Key words*: $Si_3N_4$ ceramics, high thermal conductivity, lattice oxygen content, enhancing grain growth, preparation technique*

## Introduction

The $Si_3N_4$ has been studied intensively for more than 60 years and exists in four structural phases: an amorphous a-$Si_3N_4$, and three crystalline phases, trigonal $\alpha$-$Si_3N_4$, hexagonal $\beta$-$Si_3N_4$, and a high pressure cubic $\gamma$-$Si_3N_4$ phase (or c-$Si_3N_4$), fig. 1. All basic structures are characterized by fundamental physical and chemical properties that depend mostly on production routes, compositions, micro-structures. Complete crystallization during heating, from a-$Si_3N_4$ to crystalline $\alpha$-$Si_3N_4$ runs from about 10 minutes at 1400 °C to 1 hour at 1250 °C, and to 4 hours at 1100 °C for the time-temperature domain boundary. As polycrystalline materials, $Si_3N_4$-based ceramics comprise at least of two phases, $Si_3N_4$ grains and the grain boundary. In general, it is accepted that $\alpha$-$Si_3N_4$ is the low temperature (metastable) modification, which converts to the more stable $\beta$-$Si_3N_4$ phase during high temperature sintering at normal pressure

---

[*] Corresponding author, e-mail: acavuc@vin.bg.ac.rs

[1, 2]. The synthesis of $\gamma$-$Si_3N_4$ phase with a cubic spinel structure, fig. 1(c), was carried out under high pressure (15 GPa) and at temperatures above 1920 °C in a laser-heated diamond cell [2, 3]. A $\delta$-$Si_3N_4$ phase formed in the $Si_{3.0}B_{1.1}C_{5.3}N_{3.0}$ ceramics during annealing at 1800 °C for 3 hours under a nitrogen pressure of 10 MPa [2].

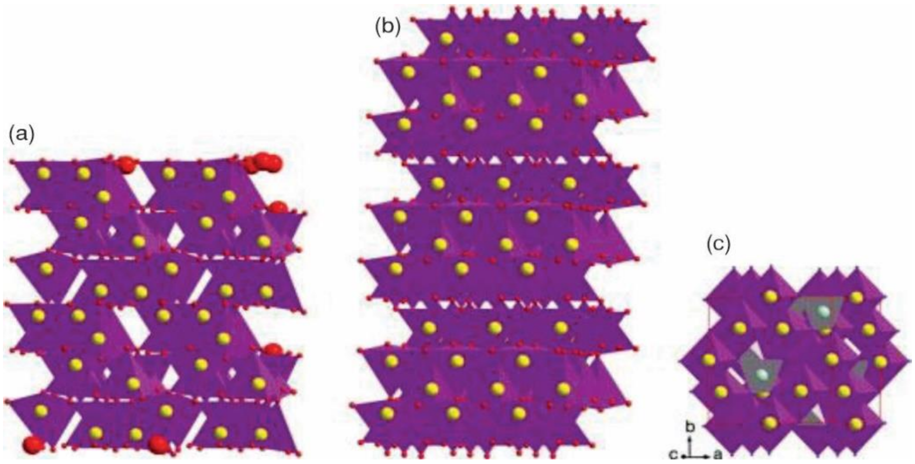

**Figure 1. Crystal structures of; (a) $\alpha$-$Si_3N_4$, (b) $\beta$-$Si_3N_4$, and (c) $\gamma$-$Si_3N_4$ [2]**

The recorded terrestrial history of $Si_3N_4$ spans just longer than 100 years. According to Lord Rayleigh's estimates it is assumed that in the earth's prehistory, when the atmosphere was chemically reducing and rich in ammonia, the crust contained large quantities of silicon and other nitrides [4].

The $Si_3N_4$ was found in nature as a mineral Nierite in the perchloric acid resistant residues of primitive meteorites (ordinary chondrites) [5] and enstatite (chondrites) [2, 6-8]. This mineral was seen to occur in size 2-0.4 µm, in lathe-shaped grains.

The $Si_3N_4$ is nowadays used as dielectric material to dissipate the heat generated from the semiconductor due to excellent electrical and thermal properties, high plasma resistance and chemical stability, high thermal conductivity which are required in electronic devices. It is also widely used in packages and substrates for IC products (*e.g.*, accelerometers, gyroscopes, pressure sensors, probe cards, large-scale integration devices, radiofrequency modules, wireless communication devices, light-emitting diodes), optoelectronic products, semiconductor power devices, and so forth [2].

## Factors influencing thermal conductivity of silicon nitride ceramics

### *Effect of impurity atoms on thermal conductivity*

The conduction of heat in dielectric ceramics like $Si_3N_4$ is governed by phonon transport: at room temperature, phonon scattering is substantially affected by imperfections in the crystal lattice, for example, impurity atoms, interstitials, and vacancies. The effect of impurities on thermal conductivities of nonmetallic crystals, was systematically investigated by Slack *et al.* [9] and revealed the strong correlation between the concentration of lattice oxygen and the thermal conductivity of single crystal [10-12]. In $Si_3N_4$ heat transfer occurs due to lattice vibration (phonon). In other words, the thermal conductivity is reduced due to the existence of lattice defects in $\beta$-$Si_3N_4$ crystals, induced by phonon scattering. It has been reported that solution of oxygen into $Si_3N_4$ crystals generates defects (vacancies) at sites of Si in crystal lattice. Lowered thermal conductivities for sintered silicon nitrides is imposed also by the addition of sintering additives resulting in distribution of low-thermal conductivity secondary phases.

Due to low self-diffusion coefficients non-oxide ceramics with high covalent bonding, such as $Si_3N_4$, AlN, and SiC even at high temperatures, are densified with the small amounts of sintering additives for development of anisotropic grains acting as reinforcements [10, 13]. The $Si_3N_4$ ceramic is well known as a high temperature structural ceramic, having high strength and high fracture toughness. Extreme hardness and toughness originate from predominantly covalent bonding and inimitable micro-structure, composed of hexagonal, rod-like grains, and bonded together reinforcing thus each other [4]. After phase transformation from α- to β-$Si_3N_4$, silicon nitride is composed of rod-like grains, reflecting the preferential growth in the [001] direction in β-$Si_3N_4$ [4]. Crack bridging as a toughening mechanism of the $Si_3N_4$ is promoted with rod-like grains acting as reinforcements as depicted in fig. 2. Improvement of mechanical properties, which go along with thermal conductivity, further increase the reliability of $Si_3N_4$ ceramics. Similarly, to fracture toughness, thermal conductivity of the $Si_3N_4$ ceramics can also be improved through micro-structure tailoring with a certain amount of large elongated grains, because large elongated grains could prolong phonon transmission paths and thus reduce scattering [13].

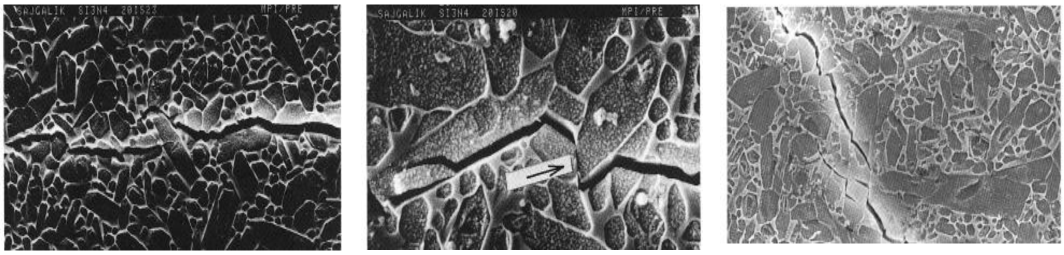

**Figure 2. Interaction of propagating crack with a thin needle-like grain β-$Si_3N_4$**

Lattice defects in β-$Si_3N_4$ grains and grain boundary phases originating from sintering additives are considered to be extrinsic factors affecting the thermal conductivity of $Si_3N_4$ [13]. A much attention has been gained to $Si_3N_4$ as a high-thermal conductivity material, with many research groups having predicted that β-$Si_3N_4$ crystal would have a high intrinsic thermal conductivity [2].

Low stability of $Si_3N_4$ at higher temperatures is overcome by densification in liquid phase in order to lower the sintering temperatures using sintering additives. Alkaline earth oxides and rare-earth oxides, are used as sintering additives for $Si_3N_4$ in a wide variety. During liquid sintering additives react with impurity oxides largely present as a surface film on the mostly α-$Si_3N_4$ nitride powder. Densification in $Si_3N_4$ to form a liquid phase is enhanced through the rearrangement of particles via solution re-precipitation reaction. During liquid-phase sintering α-to-β phase transformation promotes the development of elongated β-$Si_3N_4$ grains, fig. 2, since α-$Si_3N_4$ powder is generally used as a starting raw powder [10, 14]. Secondary phases (fractions 5-10 wt.%) thus are formed after sintering, from the liquid phase remaining in the corners of or along the matrix grains as a thin film in a form of glassy or crystalline phases.

High thermal conductive $Si_3N_4$ materials [11, 12, 15-17] should fulfill three following conditions:

- full densification of ceramics must be obtained,
- lattice oxygen content and lattice defects should be reduced in β-$Si_3N_4$ grains, since oxygen atoms located in $Si_3N_4$ lattice generate Si vacancies thus leading to phonon scattering reducing the performance of thermal conduction [10]. This reaction is explained with the following formula:

$$2SiO_2 \rightarrow Si_{Si} + 4O_N + V_{Si}$$

where $O_N$ and $V_{Si}$ is a dissolved oxygen atom in a nitrogen site and a vacancy in the Si site, respectively. A silicon vacancy is generated in order to maintain electrical neutrality, along with the substitution of O with N. The oxygen impurity from the surface of $Si_3N_4$ powder ($SiO_2$) would occupy N site in β-$Si_3N_4$ lattice during the sintering process, and the Si vacancies were formed correspondingly to retain valence balance ($O \leftrightarrow O_N + V_{Si}$) thus the mean free path of phonon decreased rapidly. According to the equation [18, 19]:

$$\kappa = \frac{C_v \bar{\text{v}} l}{3}$$

where $\kappa$ is the thermal conductivity, $C_v$ – the heat capacity, $\bar{\text{v}}$ – the phonon velocity, and $l$ – the phonon mean free path, thermal conductivity would decrease with the increase of lattice defects content. The effective approaches to decrease the lattice oxygen content in $Si_3N_4$ crystals include the selection of sintering additives with high oxygen affinity (*e.g.* rare earth oxides) [19-21], and increasing nitrogen/oxygen ratio in the liquid phase, *etc*. Nitrogen vacancy was confirmed indirectly by measuring the concentration using electron spin resonance analyses [2, 22], and

- reduced content of phases in grain boundary should also be provided. Amorphous grain boundary phases between β-$Si_3N_4$ grains, have very low thermal conductivity value (about 10-15 W/mK) and large amount of phonon scattering is introduced at the grain boundaries when the lattice vibration encounters, thus reducing the thermal conductivity performance of β-$Si_3N_4$ ceramics [23].

### *Effect of secondary phases on thermal conductivity*

In order to obtained dense $Si_3N_4$ ceramics with high thermal conductivity various oxides as sintering additives are being used during sintering react with silica impurities located as an oxidized layer mostly on the $Si_3N_4$ particle surfaces. In this way secondary phases between β-$Si_3N_4$ grains is formed resulting in distribution of low-thermal conductivity secondary phases [4]. A larger amount of sintering additive is required for $Si_3N_4$ as highly covalent compound (70% covalence) [2, 24], due to low stability under atmospheric nitrogen pressure at about 2100 K. Exception can be made when sintering via hot pressing or hot isostatic pressing (HIP). To decrease the eutectic temperatures with increasing volume fraction of the liquid phase, oxide sintering additives among alkaline-earth oxides, rare-earth oxides, alumina, zirconia, hafnia, and so on are introduced. However, effective as sintering additive for densification of $Si_3N_4$, alumina substantially decreases thermal conductivity, which is shown experimentally, due to the formation of a solid solution. Substitution Si for Al and N for O leads to formation of β-SiAlON since it dissolves into β-$Si_3N_4$ lattice. Consequently, distortion of the lattice cause the difference between the mass of a normal site and a substituted site, the thermal conductivity is reduced [10, 25, 26]. Due to formation of a solid solution (*i.e.* β-SiAlON) a variety of lattice defects for β-$Si_3N_4$ grains in sintered $Si_3N_4$ specimens are introduced like dissolution of oxygen in β-$Si_3N_4$ crystals [20, 22], dislocations [27], stacking faults [28], and precipitates inside β-$Si_3N_4$ crystals [29].

Thermal conductivity with temperature was studied systematically for $Si_3N_4$ with the variation in content of $Y_2O_3$, $Nd_2O_3$, $HfO_2$, $Yb_2O_3$, $ZrO_2$ $TiO_2$, MgO, or $Al_2O_3$ as additive [15, 30-33]. Choice of an adequate sintering additive, excluding alumina can lead to successfully fabricated $Si_3N_4$ ceramics with a higher thermal conductivity (>100 W/mK). Some of the investigated additive systems are $Y_2O_3$-$Nd_2O_3$ [25], $Y_2O_3$-$Nd_2O_3$-MgO [30], $Y_2O_3$-$HfO_2$ [16], $Yb_2O_3$-$ZrO_2$ [34], $Yb_2O_3$-MgO [35], and so forth.

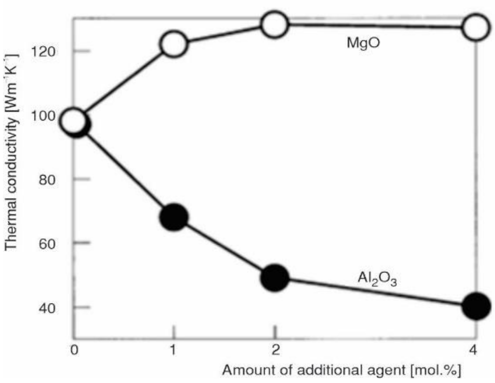

**Figure 3. The influence of MgO improved thermal conduction, while $Al_2O_3$ inhibited it [28]**

Watari *et al.* [21] obtained fully dense $Si_3N_4$ doped with 6 mol.% $Y_2O_3$ or 6 mol.% $Al_2O_3$ with capsule-HIP sintering with thermal conductivities of 70 W/mK and 20 W/mK. The highest value of the thermal conductivity, 120 W/mK was obtained for $Si_3N_4$ doped with 1 mol.% $Y_2O_3$-$Nd_2O_3$ and sintering at 2000 °C as reported by Hirosaki *et al.* [25] and Akimune *et al.* [28]. Thermal conductivity of $Si_3N_4$ doped with $Y_2O_3$-$Nd_2O_3$ was improved by addition of MgO, and drastically decreased with the further addition of $Al_2O_3$ as reported by Akimune *et al.* [28] and Okamoto *et al.* [30], fig. 3.

Duan *et al.* [19] fabricated the $Si_3N_4$ ceramics by pressure less sintering with ternary sintering additives. The highest thermal conductivity of 71 W/mK after sintering and annealing at 1810 °C/2 hours was obtained for sample $Y_2O_3$-MgO-$TiO_2$ with the mass ratio 2:3:4 and slightly increases to 74 W/mK for the prolongated dwelling time to 4 hours.

Investigating the effect of rare-earth oxides (La, Nd, Gd, Y, Yb, and Sc) on the thermal conductivity hot-pressed $\alpha$-$Si_3N_4$ powder, followed by subsequent annealing Kitayama *et al.* [35] showed that with a decreasing ionic radius of the rare-earth element, the mean grain size was increased while the lattice oxygen was decreased, and hence the thermal conductivity was increased. The obtained results in these experiments could not confirm which factor microstructure or lattice oxygen has dominant influence on thermal conductivity, because there is a close connection between the grain growth and oxygen removal. However, it was concluded based on the obtained results, that the type of rare-earth oxide additive had a significant influence on the thermal conductivity of $\beta$-$Si_3N_4$, since it depends on ionic radius, tab. 1. The larger the ionic radius of rare earth ion, the larger the activation energy for the $\alpha$-to-$\beta$ $Si_3N_4$ phase transformation, [19, 35] and the $\beta$-$Si_3N_4$ phase plays an important role in improving thermal conductivity. Thermal conductivity of the specimen increases as the ionic radius of the rare-earth element decreases, grain growth of $\beta$-$Si_3N_4$ is enhanced, lattice oxygen of $\beta$-$Si_3N_4$ grains decreases as presented in tab. 1 [19, 35].

A number of studies have been made focusing on the lattice oxygen content in $\alpha$-$Si_3N_4$ with values, ranging from 0.05 to 0.3 wt.% for pure $\alpha$-$Si_3N_4$ synthesized by chemical vapor deposition (CVD), and from 0.48 to 2 wt.% for $\alpha$-phase-rich $Si_3N_4$ ($\alpha$-phase content 80%) [23].

The relationship between thermal conductivity and lattice oxygen content for dense $\beta$-$Si_3N_4$ ceramics fabricated by hot pressing and subsequent annealing was investigated by Kitayama *et al.* [35] using various $Y_2O_3$/$SiO_2$ additive ratios. The thermal conductivity of $\beta$-$Si_3N_4$ crystals in the sintered specimens was estimated using a modification of the Wiener method in order to exclude microstructural factors such as grain size and the number of grain boundaries.

**Table 1. Thermal conductivities of and lattice oxygen contents for samples sintered with different rare earth oxide additives**

| Additive | Ionic radius [nm] | Annealing time [hours] | Lattice oxygen [%] | Thermal conductivity [$Wm^{-1}K^{-1}$] | Thermal diffusivity [$m^2s^{-1}$] | Density [$gcm^{-3}$] | Grain size [μm] |
|---|---|---|---|---|---|---|---|
| | | | | Para Perp | Para Perp | | Para Perp |
| $Sc_2O_3$ | 0.73 | 4 | 0.0851±0.0038 | 84.9 100.8 | 0.38 0.45 | 3.231 | 3.61 3.46 |
| | | 16 | 0.0775±0.0035 | 89.6 106.3 | 0.40 0.47 | 3.198 | 4.57 4.44 |
| $Yb_2O_3$ | 0.86 | 4 | 0.0615±0.0022 | 86.1 115.0 | 0.36 0.47 | 3.462 | 3.85 3.73 |
| | | 16 | 0.0802±0.0065 | 88.6 114.7 | 0.37 0.48 | 3.442 | 3.94 3.64 |
| $Y_2O_3$ | 0.89 | 4 | 0.0765±0.0013 | 82.9 104.6 | 0.36 0.46 | 3.252 | 4.58 4.16 |
| | | 16 | 0.0632±0.0018 | 82.7 105.8 | 0.36 0.46 | 3.277 | 4.79 4.25 |
| $Gd_2O_3$ | 0.94 | 4 | 0.0692±0.0126 | 78.7 100.7 | 0.33 0.42 | 3.421 | 4.14 3.78 |
| | | 16 | 0.0765±0.0013 | 81.6 106.9 | 0.34 0.45 | 3.420 | 4.74 4.00 |
| $Nd_2O_3$ | 1.00 | 4 | 0.0942±0.0045 | 64.1 81.6 | 0.27 0.34 | 3.396 | 1.24 0.85 |
| | | 16 | 0.0923±0.0134 | 72.2 97.9 | 0.31 0.41 | 3.379 | 2.39 2.06 |
| $La_2O_3$ | 1.06 | 4 | 0.2794±0.0371 | 28.1 31.6 | 0.12 0.13 | 3.351 | N/A N/A |
| | | 16 | 0.1163±0.0055 | 51.1 64.9 | 0.22 0.28 | 3.327 | 1.38 1.27 |

Kanzaki *et al.* [27] used a hot-gas extraction method to determine the oxygen content in β-$Si_3N_4$ crystal lattices that originally had been developed for measuring the lattice oxygen in an AlN crystal [36]. Crystals of β-$Si_3N_4$ were fabricated using α-$Si_3N_4$, $Y_2O_3$, and $SiO_2$ with molar ratios of 20:1:2 and 20:2:1 $Y_2O_3$-$SiO_2$ as additives ($Y_2O_3$:$SiO_2$ 1 : 2 or 2 : 1) by heat treatment of α-$Si_3N_4$ (SN-E05 Grade, aluminum content of <50 ppm, UBE Industries, Ltd., Yamaguchi, Japan) as a raw powder. The acid rinse treatment was used to remove any secondary phases. Depending on the composition of the liquid phase the lattice oxygen contents in the β-$Si_3N_4$ crystal were reported as 0.258 wt.% (in the case of $Y_2O_3$:$SiO_2$ 1 : 2) and 0.158 wt.% (in the case of $Y_2O_3$: $SiO_2$ 2:1). Performance of thermal conduction would be expected to be lower due to the dissolution of oxygen into the β-$Si_3N_4$ a large number of lattice vacancies is formed leading to phonon scattering.

Secondary phases in $Si_3N_4$ ceramics formed after sintering, from the liquid phase remaining in the corners as a thin film of or along the matrix grains as grain boundary phases in addition to the lattice oxygen content, negatively affects the thermal conductivity, fig. 4.

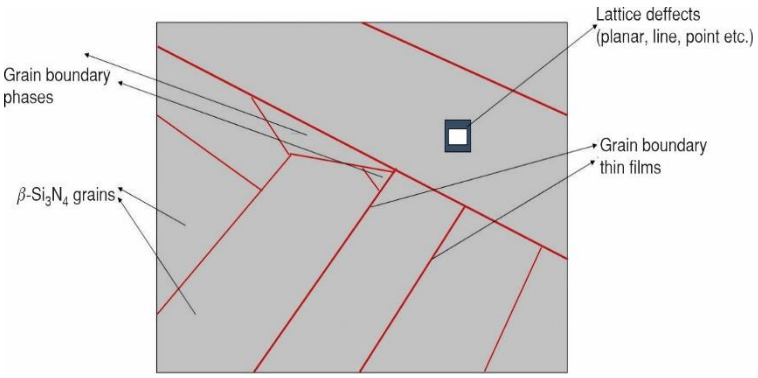

**Figure 4. Micro-structural factors of $Si_3N_4$ ceramic affecting thermal conductivity**

Thermal conductivities of grain boundary phases are 1-2 orders of magnitude lower than pure $Si_3N_4$ crystals like of yttrium aluminate (typical secondary phase in AlN with $Y_2O_3$ addition) and oxynitride glass (typical secondary phase in $Si_3N_4$) are about 10 W/mK and 1 W/mK. Morphology distribution as a continuous film around the matrix grains substantially lowers the thermal conductivity, while isolated distribution in a form of pockets does not distinctly affect the thermal conductivity.

Owing to the well-faceted grains with a rod like shape, micro-structure of $Si_3N_4$ ceramic is more complicated, secondary phase is generally presented as a glassy phase surrounding the matrix grains, fig. 4, mostly because the liquid phase contains $SiO_2$ which is difficult to crystallize perfectly. Negative effect of the secondary phase on thermal conductivity is even more pronounced between two grains in $Si_3N_4$ ceramic since distribution of glassy phase is not only as pockets surrounded by β-$Si_3N_4$ grains, but also in the openings. Because β-$Si_3N_4$ grains have prismatic planes and are inclined to each other in most parts grain boundary thin films present between two-grain junctions with an equilibrium thickness (typically 1-2 nm) [37]. The other parts should have greater inter-grain equilibrium thickness in liquid-phase-sintered $Si_3N_4$ ceramic.

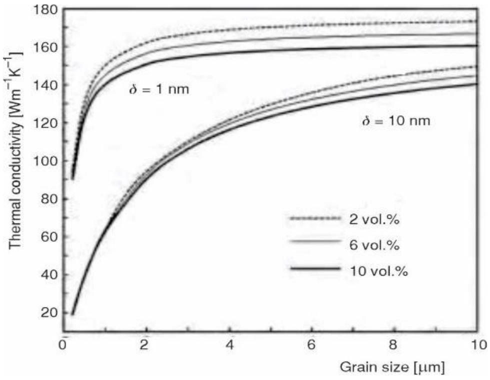

**Figure 5. Effect of volume fraction of glassy phase on thermal conductivity of β-$Si_3N_4$ for *R* (aspect ratio) = 1 in β-grain and $\delta$ = 1 and 10 nm [2]**

The thermal conductivity of β-$Si_3N_4$ ceramic having grain-boundary films of a few nanometers thickness decreases quickly as the size of the β-$Si_3N_4$ grains decreases to less than 1 μm according to calculation based on a simple modified Wiener's model [38] for the thermal conductivity of a composite material [39]. Calculation of the effect of the volume fraction of the glassy phase on the thermal conductivity of $Si_3N_4$ ceramics, with the aspect ratio of $Si_3N_4$ being 1, is illustrated in fig. 5.

The calculation indicated that thermal conductivity of the β-$Si_3N_4$ crystal and the glassy phase if grain boundary thickness, $\delta$, was 1 and 10 nm, were 180 W/mK and 140 W/mK, respectively. So, the thermal conductivity of $Si_3N_4$ ceramic is heavily dependent on the average grain boundary film thickness, which was in the range of a few tenths of a nanometer. When the grain boundary thickness was 1 nm the thermal conductivity of $Si_3N_4$ initially increased steeply with increasing grain size up to certain extent, to reach constant values determined by the film thickness and the amount of glassy phase. When the grain size exceeds certain critical values (about 1 μm), grain-boundary thin films have little effect on the thermal conductivity of $Si_3N_4$, as shown in fig. 5. As for now, in addition to the role of purifying the β-$Si_3N_4$ lattice, grain growth is necessary in order to improve the thermal conductivity of $Si_3N_4$ ceramic.

### *Improvements in thermal conductivity for silicon nitride ceramics*

Increasing sintering time is one of the ways to improve the thermal conductivity of $Si_3N_4$ ceramics in order to a reduce number of two-grain junctions [25, 39], but also to the purification of grains [16] because of grain growth via solution-reprecipitation processes. Improvement of $Si_3N_4$ thermal conductivity doped with 2 mol.% MgO-5 mol.% $Yb_2O_3$ was done by Hayshi *et al.* [40], or with 1 wt.% $HfO_2$-8 wt.% $Y_2O_3$ by Yokota *et al.* [17] after sintered at

2273 K for between 2 and 48 hours. In both experiments, β-$Si_3N_4$ were used as a raw powder in order to exclude the effect of any α-to-β phase transformation. The thermal conductivities were increased with increasing sintering time because of appreciable grain growth and decrease in lattice oxygen content in the β-$Si_3N_4$ grains [40]. Yokota *et al.* [17] doped $Si_3N_4$ with $HfO_2$-$Y_2O_3$ additives and sintered at 2273 K for 8 and 48 hours, and obtained materials with increased thermal conductivities from 88 and 120 W/mK.

In both specimens, a bimodal micro-structure where larger elongated grains with a grain diameter in excess of 2 µm were dispersed in fine matrix grains was obtained. As expected, specimen sintered for 48 hours had higher volume fraction of the larger grains compared to the specimen sintered for 8 hours. Why grain growth is so important regarding amount of impurity oxygen is experimentally confirmed, a minimal change in lattice oxygen content of the smaller matrix grains was measured between 8 and 48 hours (1900 ppm for 8 hours and 1920 ppm for 48 hours). There was a drastic decrease in contrast in the lattice oxygen content of larger, elongated grains (980 ppm for 8 hours and 460 ppm for 48 hours). Due to a higher affinity for oxygen in $Y_2O_3$ containing oxynitride glassy phase, the purification of β-$Si_3N_4$ grains occurs through a dissolution–reprecipitation process during long-term heating. Thus, the thermal conductivity of $Si_3N_4$ ceramic was increased with increasing amounts of purified larger grains [17].

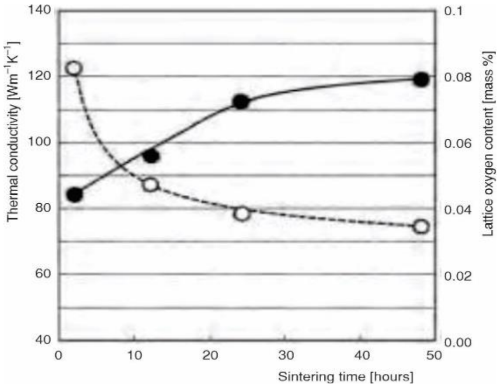

**Figure 6. Variation of thermal conductivity and lattice oxygen content with sintering time for the $Si_3N_4$ specimens doped with 2 mol.% MgO-5 mol.% $Yb_2O_3$ sintered at 2173 K under 0.9 MPa $N_2$ [2]**

As already mentioned, there is a clear tendency for thermal resistivity tends to decrease, with a decreasing lattice oxygen content in the β-$Si_3N_4$ though the additive system, type of raw $Si_3N_4$ powder and processing method, were different among mentioned investigations, fig. 6. Literature data showed that the β-$Si_3N_4$ free of lattice oxygen exhibit a thermal conductivity of at least 180 W/mK. To enhance the thermal conductivity, sintering additives should play a dual role of promoting densification and removing lattice oxygen. Ratio of additive oxide to $SiO_2$ existing in a raw $Si_3N_4$ powder would also affect the thermal conductivity of the sintered specimens showing tendency to increase with increasing $Y_2O_3$:$SiO_2$ ratio, with a significant rise occurring when the ratio was close to 1 by Kitayama *et al.* [20]. He fabricated $Si_3N_4$ with various $Y_2O_3$/$SiO_2$ additive ratios (0.289, 0.807, 1.267, and 2.029) by hot pressing. The same effect occurring with $Y_2O_3$-doped AlN proposed by Jackson *et al.* [41] explains the effect of grain-boundary composition on the thermal conductivity of $Y_2O_3$-doped $Si_3N_4$. There is a three-phase field with an increasing $Y_2O_3$:$SiO_2$ ratio, shifting from Region I ($Si_3N_4$-$Si_2N_2O$-$Y_2Si_2O_7$), to Region II ($Si_3N_4$-$Y_2Si_2O_7$-$Y_{20}N_4Si_{12}O_{48}$), and finally to Region III ($Si_3N_4$-$Y_{20}N_4Si_{12}O_{48}$-$Y_2Si_3N_4O_3$).

The activity of $SiO_2$ was decreased in the order of Regions I-III in corresponding with the variant of the three-phase field. Oxygen content of β-$Si_3N_4$ lattice, depending on $SiO_2$ activity, dictated the grain-boundary phase composition at the three-phase field. The solubility of oxygen in β-$Si_3N_4$ was the lower as the activity of $SiO_2$ was lower in the three-phase field. When both the $Y_{20}N_4Si_{12}O_{48}$ and $Y_2Si_3N_4O_3$ phases were present in the grain-boundary phase simultaneously, the highest thermal conductivity was achieved.

One of the effective ways of improving the thermal conductivity of $Si_3N_4$ considering the amount of oxygen in the grain-boundary glassy phase, is to use of a nitride instead of oxide sintering additive. Hayashi *et al*. [40] measured the lattice oxygen content of the β-$Si_3N_4$ grains and thermal conductivity in compacts of β-$Si_3N_4$ raw powder doped with either MgO-$Yb_2O_3$ or $MgSiN_2$-$Yb_2O_3$ as an additives, sintered at 2173 K for 2 to 48 hours under a 0.9 MPa nitrogen pressure. Specimen in which $MgSiN_2$ was used as additive a magnesium supply source a non-oxide, exhibited a lower lattice oxygen content, and thus a higher thermal conductivity for about 20 W/mK higher than that of the MgO-doped $Si_3N_4$, and reached a maximum of over 140 W/mK following a 48 hours period of sintering, fig. 6. The purification of $Si_3N_4$ grains via a solution-reprecipitation process in the nitrogen-rich grain boundary glassy phase was provided by $MgSiN_2$ as non-oxide additive and as consequence higher thermal conductivity $Si_3N_4$ and enhanced grain growth that had resulted in a micro-structure where the larger grains were in contact with each other. Improved thermal conductivity of $Si_3N_4$ ceramics thus is related to removal of the lattice oxygen by using high purity β-$Si_3N_4$ or Si raw materials with effective sintering additives and high temperature sintering/annealing processes. In order to achieve improved thermal conductivities, over 100 W/mK in untextured $Si_3N_4$, where elongated β-$Si_3N_4$ grains are randomly aligned much effort has been made [12, 13, 25, 27, 42, 43]. Thermal conductivity of 177 W/mK was obtained by sintering of reaction bonded $Si_3N_4$ (RBSN) heated at 1900 ˚C for 60 hours, followed by cooling at a very low rate of 0.2 °C per minute an untextured $Si_3N_4$ was obtained as reported by Zhou *et al.* [44], since the thermal conductivity of β-$Si_3N_4$ is intrinsically anisotropic with a thermal anisotropy as high as 450/170 (thermal conductivity along *c*- and *a*-axis) = 2.6. A self-reinforced $Si_3N_4$ ceramic with high thermal conductivity was prepared by Kong *et al*. [46] through multi-step pressure less sintering with $Y_2O_3$ and MgO additives. A bimodal micro-structure is established by the steps consisted of phase control and densification stages to provide additional crystallization sites using a partial α-to-β phase transformation. Specific phase transformation and linear shrinkage that occurred at 1400 °C enabled the best mechanical and thermal properties, flexural strength of 932 MPa and thermal conductivity of 74 W/mK.

### *Harmonic improvement of thermal conductivity and mechanical properties*

The relationship between grain size and thermal conductivity can be established by calculated phonon mean free path for the sintered materials. If the phonons are scattered significantly by the presence of grain boundary, the phonon mean free path must equal the magnitude of the grain size. However, the grains of the samples were too large compared with the phonon mean free path. Hence, the thermal conductivity of $Si_3N_4$ ceramics must not be controlled only by the grain size. Thermal conductivities of the samples were enhanced as the frequencies of the large grains increased [46]. Enhance grain growth of β-$Si_3N_4$ grains throughout dissolution-reprecipitation process decreases the lattice oxygen thus leading to improved thermal conductivity of $Si_3N_4$ ceramics.

Grain growth further participates in reducing the number of grain boundary glassy phases between two β-$Si_3N_4$ grains and increase thermal conductivity of $Si_3N_4$. Approach set in this way is only beneficial for a critical value of grain size, below a few microns [39]. In order to achieve grain purification, gas-pressure sintering is common way for fabrication of high-thermal conductivity (>100 W/mK) $Si_3N_4$ ceramics at temperatures of about 2173 K for an unusually long period of time (1-2 days), or at temperatures in excess of 2373 K under high $N_2$ pressures (>10 MPa) for several hours [47]. Obtained material, however, has very poor mechanical properties originated from coarse micro-structure. As already mentioned, due to low self-diffusion coefficients non-oxide ceramics such as $Si_3N_4$ with high covalent bonding, at high temperatures, are densified with the small amounts of sintering additives, which promote development of anisotropic grains acting as reinforcements. The effect of anisotropic grains acting as reinforcements using seeding is a useful method and bimodal micro-structure on mechanical properties, fig. 7, and thermal conductivity of $Si_3N_4$ ceramic was widely studied by many authors [14, 48, 49].

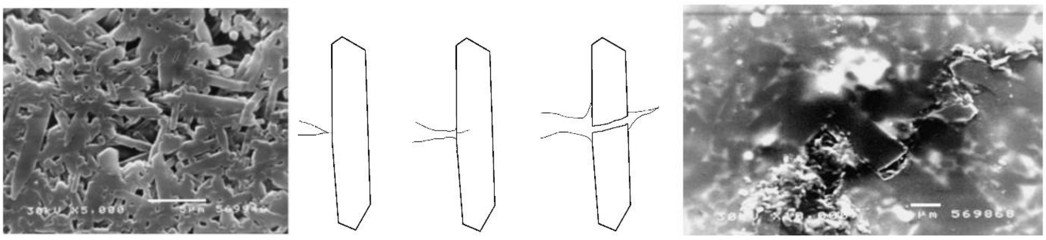

**Figure 7. The SEM photograph of the polished and chemically etched surface of silicon nitrides sintered at; 1800 °C for 4 hours with 3 wt.% β-$Si_3N_4$ seed particles (a), schematic representation of crack propagation (b), and SEM photograph of the silicon nitrides with 3 wt.% β-$Si_3N_4$ seed particles showing the propagating crack (c) [48]**

One of the ways to improve mechanical properties along with thermal conductivity and to further increase the reliability of $Si_3N_4$ has shifted the emphasis towards seeding and prolonging sintering time in an attempt to grow further the elongated uniformly distributed grains in a matrix of equiaxed or slightly elongated grains thus forming bimodal micro-structure. By incorporating a controlled amount of elongated β-$Si_3N_4$ single crystal particles into the matrix, toughening mechanisms such as crack deflection and/or bridging via interfacial debonding, are activated, figs. 7(b) and 7(c). It is now well accepted that seeding is a useful method of providing an effective way to improve the fracture resistance while retaining high strength, provided that the size, content and distribution of the elongated β-$Si_3N_4$ single-crystal particles are carefully controlled [48]. Figure 7(a) and 7(c) shows the SEM photograph of the polished and chemically etched surface of silicon nitrides sintered at 1800 °C for 4 hours with 3 wt.% β-$Si_3N_4$ seed particles. Seeded samples, as expected, exhibit a bimodal micro-structure of large rod-like grains embedded in a small matrix grain [48].

### *High thermal conductivity through reaction bonding and post sintering*

Another approach to improved thermal conductivity of $Si_3N_4$ is to apply a reaction bonding (RB) process. The $Si_3N_4$ ceramics from a Si powder compact are usually fabricate this way [50]. Reducing the impurities in raw silicon powder to an extremely low level was noted in 1995 by Haggerty [51]. Leading to that improved thermal conductivity of reaction-bonded $Si_3N_4$. High-thermal conductivity silicon nitrides by sintering of reaction-bonded silicon nitride (RBSN) were investigated by a research group at the National Institute of Advanced Industrial Science & Technology, in Japan [2, 42, 47, 52, 53].

A $Si_3N_4$ compact is formed when a Si powder compact is heated at about 1673 K in a nitrogen atmosphere. The external dimensions of the compact are retained as the individual Si particles expands by about 22%, and nitridation reaction proceeds (mainly via a gas-solid reaction system) [50]. The RB process offers following improvements:

- rather than the more expensive $Si_3N_4$ powder a cheaper Si powder can be used as the starting material and

- because of the higher density of the pre-sintered specimens shrinkages accompanied by post-sintering can be minimized.

Starting with the pre-sintered specimen with a finer micro-structure and a higher density which favorable for controlling the micro-structure of the final product RB process provides fabricating high-performance silicon nitride ceramics.

The RB and post sintering has been known as a fabrication process of dense $Si_3N_4$ sintered body where Si powder compact is heat-treated in nitrogen atmosphere for transformation into $Si_3N_4$ and post-sintered [50, 54]. For full densification by this approach, the nitridation and post-sintering are carried out in an inert atmosphere, leading to substantial reduction in the impurity oxygen content [55]. Furthermore, even coarse Si powder is decomposed into fine $Si_3N_4$ powder in nitridation as shown, thus facilitating full densification during the post sintering [47, 53, 54]. As starting, raw powder a high purity Si powder with an oxygen content of 0.28 wt.%, a total metallic impurity content of <0.01 wt.%, and a mean particle size (d50) of 50 8.5 µm was used [54]. As sintering additives during post-sintering high purity 2 mol.% $Y_2O_3$-5 mol% MgO were added to the Si powder, and were mixed in methanol using a planetary mill. The oxygen content of Si powders after planetary milling increased from 0.28 wt.% to 0.51 wt.%, which was still relatively low compared to those of the commercial high-purity $Si_3N_4$ powders (typically 1 wt.% or higher). Sintered RBSN (SRBSN) which was obtained through reaction-bonding (nitridation) at 1400 °C for 8 hours under 0.1 MPa nitrogen pressure and post-sintering at 1900 °C for 12 hours under 0.9 MPa nitrogen pressure had large fibrous grains embedded in fine grain matrix without pores. For comparison, micro-structure of gas-pressure sintered silicon nitride (GPSSN) obtained under the same sintering conditions using a commercial high-purity $Si_3N_4$ powder (mean particle size: 0.2 µm, oxygen content: 1.2 wt.%) [47, 53, 54].

Due to a smaller amount of impurity oxygen contained in the starting powder although similar micro-structures, the thermal conductivity of the SRBSN is 120 W/mK, which was about 20% higher than that of the GPSSN, 98 W/mK. So, it was confirmed that with increasing the sintering time, the thermal conductivity increases for all the samples due to grain coarsening and diffusion of lattice oxygen into grain boundaries [55]. Also, the SRBSN shows both high strength and high thermal conductivity compared to the GPSSN. Zhou, *et al.* [55] investigated in detail the effects of nitridation conditions on the properties of the nitrided and post-sintered samples.

Authors confirmed that via controlling the nitrogen atmosphere further improvement of the thermal conductivity is possible by increasing $\beta/\alpha$ phase ratio of the nitrided sample from conventional 60:40 to 83:17, since it is known that an amount of oxygen solved into $\beta$-$Si_3N_4$ is smaller than that into $\alpha$-$Si_3N_4$ [55]. Lowered thermal conductivity due to the content of lattice oxygen, could be reduced also by enhanced grain growth via a solution-reprecipitation process not only by reaction with sintering additives to form stable compounds at the grain boundaries. Thermal conductivity of $\beta$-$Si_3N_4$ ceramics is affected by micro-structural factors the, such as porosity, grain size (particularly large elongated grain size) [10].

Zhu *et al.* [53] investigated the effect of the impurity oxygen content of raw Si powder on the properties of a RBSN ceramic using A (finer) and B (coarser) powder. But these micro-structure factors are not responsible for the difference in the thermal conductivity between the A (finer) and B (coarser) powder samples, owing to the following facts:

- the former shows more complete densification than the latter,
- the former shows more pronounced large elongated $\beta$-$Si_3N_4$ grain growth than the latter, which is inconsistent with the previous reports that the thermal conductivity of $\beta$-$Si_3N_4$

ceramics increases with increased fraction of large grains as a result of the increased contiguity of β-$Si_3N_4$-β-$Si_3N_4$ [16, 17, 25, 30, 34, 40], and
- although the former shows a slightly higher amount of secondary phases than the latter, the secondary phases in both the samples are principally located at the triple grain–boundary junction.

This distribution makes the secondary phases less harmful to the thermal conductivity of β-$Si_3N_4$ ceramics [15]. Therefore, the reason why the B (coarser) powder sample shows higher thermal conductivity than the A (finer) powder sample is mainly attributed to lesser lattice defects in the former, due to the native oxygen content and the least level of aluminum impurity from the raw powder. It is of interest to see that there is no difference in the thermal conductivity between the A powder samples sintered from the nitrided bodies at 1350 °C and 1400 °C, suggesting that the nitriding temperature has no effect on the thermal conductivity of SRBSN [53]. On the one hand, the nitriding temperature does not affect the β-$Si_3N_4$ grain growth via a solution-reprecipitation process during post-sintering, so it most likely does not affect the removal of lattice oxygen in β-$Si_3N_4$. On the other hand, considering that the dissolved Al in β-$Si_3N_4$ is stable during sintering, it is believed that the nitriding temperature has no effect on the removal of the dissolved Al in β-$Si_3N_4$ during post sintering. As a result, the same thermal conductivity is due to the similar micro-structure as well as the similar lattice defects between them. It is interesting to see that the thermal conductivity of the SSN material appears almost the same as that of the SRBSN material but is lower than that of the SRBSN material prepared from B (coarser) powder [53]. This is because the high-purity coarse Si powder with several micrometers, even with a few tenths of a micrometer, is feasible for producing dense SRBSN materials, which is beneficial for further reducing the cost of production, because the nitridation makes them convert into sub-micro sized and even nanosized $Si_3N_4$ products [56, 57]. From the stand point of enhancing the thermal conductivity of SRBSN, the present work suggests that further decreasing the particle size is unnecessary for the following reasons:
- the prolonged milling process invariably introduces greater amounts of both extraneous aluminum impurity and oxygen, which may be harmful to thermal conductivity of SRBSN and
- complete nitridation can be achieved at a temperature near the melting point of Si, 1400 °C.

The property evaluation reveals that the coarse Si powder leads to a higher thermal conductivity of SRBSN than the fine Si powder, which is attributed to the lower amounts of native oxygen and aluminum impurities.

However, the nitriding temperature has no effect on the thermal conductivity of SRBSN and this is in agreement with the similar micro-structure as well as the similar lattice defects. This work demonstrates that the improvement in high thermal conductivity of SRBSN materials could be achieved by using a coarse Si powder with lower amounts of native oxygen and aluminum impurity [56].

### *Anisotropic thermal conductivity in textured $Si_3N_4$*

Due to its strong intrinsic thermal anisotropy the formation of a textured micro-structure is necessary to obtain $Si_3N_4$ ceramics with high thermal conductivities. Control of the amount of oxygen impurity which depend on the sintering additives and the degree of texture depending on texturing method used, is decisive to enhance the thermal conductivity of textured $Si_3N_4$, respectively, [43, 58]. Development of textured micro-structure in which the elongated β-$Si_3N_4$ grains are oriented almost unidirectional as shown in fig. 8 is another approach to achieve a high thermal conductivity in $Si_3N_4$ ceramic. Because of the much higher thermal

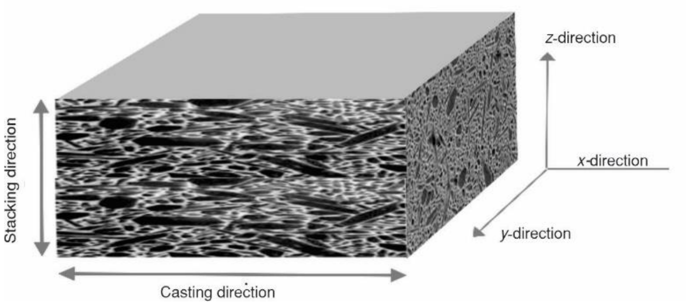

**Figure 8. Micro-structure of seeded and tape-cast $Si_3N_4$ (left-hand side) and three different directions for thermal conductivity measurements (right-hand side)**

conductivity along the *c*-axis than along the *a*-axis in β-$Si_3N_4$ crystals a high thermal conductivity along the grain orientation would be expected, compared to a material with a random distribution of β-$Si_3N_4$ grains [18, 59]. Forming process generating shear stress, such as tape-casting and extrusion in a combination of the seeding of rod-like β-$Si_3N_4$ nuclei enables the fabrication of anisotropic micro-structures [60-62]. This process is based on the grain-growth behavior of $Si_3N_4$ during the α-to-β phase transformation, with the preferential nucleation site of the newly formed β-$Si_3N_4$ phase on pre-existing β particles. After the transformation only few α and large β grains will be distributed selectively particularly along the *c*-axis direction, via a solution-reprecipitation reaction. The typical micro-structure of seeded and extruded $Si_3N_4$ is shown in fig. 8 [2, 63]. The method of adding large β-$Si_3N_4$ grains to the raw $Si_3N_4$ powder by grain growth of $Si_3N_4$ crystals in polycrystalline ceramics improves thermal conductivity due to purification of the grains while decreasing the two-grain junction films. Introducing large β-$Si_3N_4$ particles as seeds into fine $Si_3N_4$ raw powder is also effective in controlling the micro-structure. During firing, fine $Si_3N_4$ dissolves and precipitates on the large β-$Si_3N_4$ particles. Seeds addition accelerates grain growth because difference in grain size is driving force for grain growth. Seeds addition increased the thermal conductivity up to 122 W/mK, under the condition of heat-treatment at 2000 °C. Grain growth not only decreases the amount of films, but also decreases amount of impurities and defects in $Si_3N_4$ grains because $Si_3N_4$ raw powders contain impurities and crystal defects in the grain. The grown parts of $Si_3N_4$ grain have a lower amount of impurities and defects than the raw $Si_3N_4$ powder because most of impurities and defects in the raw powder are removed by the segregation phenomena at the precipitation step during the liquid phase sintering in which smaller $Si_3N_4$ grains dissolve to the liquid, diffuse in the liquid, and reprecipitate onto the larger grains. Therefore, the material with large grain size has higher thermal conductivity [28]. Yang *et al.* [13] fabricated high thermal conductive β-silicon nitride (β-$Si_3N_4$) ceramics from fine α-$Si_3N_4$ powder as the raw material and coarse β-$Si_3N_4$ particles as the nuclei through spark plasma sintering at 1650 °C for 5 minutes and post-sintering heat treatment at 1900 °C for 4 hours. The thermal conductivity of the sample with 10 mol.% of β-$Si_3N_4$ nuclei reached a maximum value of 84.6 W/mK. These results revealed that the thermal conductivity of β-$Si_3N_4$ ceramics was independent of the grain size and controlled by the amount of reprecipitated large grains.

The material exhibits a high anisotropy where the large elongated grains, which are grown from seeds, are almost unidirectional oriented parallel to the forming process which is used. The thermal conductivities are measured in three different directions, as shown in fig. 8, [10]. As expected, for each of these specimens the thermal conductivity was highest along the grain alignment. The anisotropic properties result from the orientation of elongated β-$Si_3N_4$ grains or its combination with intrinsic anisotropic properties of β-$Si_3N_4$. The intrinsic thermal conductivity (ideal crystal: 170 W/mK (*a*-axis) and 450 W/mK (*c*-axis) [18] allows the texturing to efficiently improve thermal conductivity of $Si_3N_4$ ceramics [63]. In particular, a highly anisotropic $Si_3N_4$ with very long grains and fabricated under extreme conditions, exhibited a high thermal conductivity of about 150 W/mK in the direction parallel to the grain alignment [62]. In recent times, further improvements are made with strong magnetic field alignment (SMFA) as a novel and potential technique for the near-net-shape production of textured $Si_3N_4$ with the *c*-axis parallel to the thickness direction. This technique has no limitations to the particle morphology of the raw powder and has two key requirements:

- the material should exhibit the magnetic anisotropy, normally with a non-cubic crystal structure and
- the suspension should be well deagglomerated to allow the orientation of single crystals [64].

A rotating strong magnetic field (RSMF) is one solution to achieve the *c*-axis orientation, and this is practically conducted by rotating the sample in a horizontal static strong magnetic field and has been used to produce *c*-axis textured ceramics such as $Si_3N_4$ [58]. Highly textured ceramics by colloidal processing can be simply obtain in a SMFA as confirmed by Sakka *et al*. [64, 65].

Zhu *et al*. [43, 58, 66] propose a strategy for fabricating textured $Si_3N_4$ with high thermal conductivity of over 170 W/mK along the grain alignment direction by slip casting α-$Si_3N_4$ raw powder with β-$Si_3N_4$ seeds and $Y_2O_3$-$MgSiN_2$ [11] as sintering additives in an RSMF in a RSMF of 12 *T*, followed by gas pressure sintering at 1900 °C for 12 hours at 1 MPa pressure in nitrogen. Zhu *et al*. [66] further investigate the *c*-axis texture development and thermal conductivity in seeded $Si_3N_4$, with a thermal anisotropy of 2.2 for β-$Si_3N_4$ whiskers by slip casting in an RSMF. The thermal conductivity in the directions parallel and perpendicular to the slip casting direction, corresponding to 29 W/mK and 30 W/mK, respectively, indicating the thermal isotropy. However, the c-axis oriented sample exhibits 25 W/mK and 51 W/mK in the directions parallel and perpendicular to the rotating magnetic field, *i.e*., perpendicular and parallel to the *c*-axis of β-$Si_3N_4$ grains [66].

## Summary and outlook

Amounts of lattice oxygen and grain boundary phase, textured $Si_3N_4$ as the most important factors affecting the thermal conductivity of $Si_3N_4$ ceramics were reviewed in in this paper. Much research has been carried out in order to improve thermal conductivity using of variety of production methods. This review has mainly focused on the effects of sintering additives and the forming and sintering processes on the thermal conductivity of $Si_3N_4$ ceramics. Some clear conclusions can be draw summarizing the presented research results:

- the addition of non-oxide sintering additives tends to improve the thermal conductivity of $Si_3N_4$ ceramics comparing to oxide sintering additives,
- the growth of β-$Si_3N_4$ grains is promoted with increase in sintering temperature and holding time, and the oxygen content of the crystal lattice is continuously reduced by the process of dissolving-precipitate, thereby promoting the increase of thermal conductivity, and
- the orientation of β- $Si_3N_4$ grains in textured $Si_3N_4$ ceramics affects the thermal conductivity of $Si_3N_4$ ceramics in different directions parallel and perpendicular to the grain alignment.

For practical use of highly-thermal-conductive $Si_3N_4$ ceramic, many problems still need to be solved, like development of low-cost technology. Currently used preparation methods are time-consuming and require high temperature heat treatments, and thus are expensive. Special attention for the future research should be paid on how to control the effects of lattice oxygen and grain boundary phases at lower temperatures and shorter holding times and how to reduce the sintering temperature. Finally, development of high thermal conductivity of silicon nitride ceramics should correlate with improved mechanical properties.

## Acknowledgment

The authors would like to thank Ministry of Science, Technological Development and Innovation of the Republic of Serbia for financial support under Grant No. 451-03-68/2022-14/200017 and 451-03-47/2023-01/200051.

## References

[1] Grun, R., The Crystal Structure of β-$Si_3N_4$: Structural and Stability Considerations Between α- and β-$Si_3N_4$, *Acta Crystallographica Sect. B Struc. Crystallography and Cry. Chem., 35* (1979), 4, pp. 800-804
[2] Riedel, R., *et al*., *Ceramics Science and Technology*, Wiley-VCH, Weinheim, Germany, 2008
[3] Zerr, A., *et al*., Synthesis of Cubic Silicon Nitride, *Nature, 400* (1999), July, pp. 340-342
[4] Riley, F. L., Silicon Nitride and Related Materials, *J. of the Amer. C. Soc., 83* (2000), 2, pp. 245-265
[5] Alexander, C. M. O., *et al*., SiC, and $Si_3N_4$ in Qingzhen (EH3), Lunar and Planetary Institute, McDonnell Center for the Space Sciences, Washington University, St Louis, Mo., USA, 1991
[6] Alexander, C. M. O., *et al*., Occurrence and Implications of Silicon Nitride in Enstatite Chondrites, *Meteoritics, 29* (1994), 1, pp. 79-85
[7] Stone, J., *et al*., Correlated Si Isotope Anomalies and Large13C Enrichments in a Family of Exotic SiC Grains, *Earth and Planetary Science Letters, 107* (1991), 3-4, pp. 570-581
[8] Lee, M. R., *et al*., Nierite ($Si_3N_4$), a New Mineral from Ordinary and Enstatite Chondrites, *Meteoritics, 30* (1995), 4, pp. 387-398
[9] Slack, G. A., Nonmetallic Crystals with High Thermal Conductivity, *Journal of Physics and Chemistry of Solids, 34* (1973), 2, pp. 321-335
[10] Hirao, K., *et al*., High Thermal Conductivity Silicon Nitride Ceramic, *MRS Bulletin, 26* (2001), June, pp. 451-455
[11] Zhu, X., *et al*., Influence of Additive Composition on Thermal and Mechanical Properties of β-$Si_3N_4$ Ceramics, *J. Mater. Res. 19* (2004), Nov., pp. 3270-3278
[12] Zhu, X., *et al*., Potential use of Only $Yb_2O_3$ in Producing Dense $Si_3N_4$ Ceramics with High Thermal Conductivity by Gas Pressure Sintering, *Science and Tech. of Advanced Materials, 11* (2010) 065001
[13] Yang, C., *et al*., Micro-structure Tailoring of High Thermal Conductive Silicon Nitride Through Addition of Nuclei with Spark Plasma Sintering and Post-Sintering Heat Treatment, J*ournal of Alloys and Compounds, 785* (2019), May, pp. 89-95
[14] Lange, F. F., Fracture Toughness of $Si_3N_4$ as a Function of the Initial α-Phase Content, *Journal of the American Ceramic Society, 62* (1979), 7-8, pp. 428-430
[15] Kim, J.-M., *et al.*, Effects of Micro-structure and Intergranular Glassy Phases on Thermal Conductivity of Silicon Nitride, *Ceramics International, 43* (2017), 7, pp. 5441-5449
[16] Yokota, H., Ibukiyama, M., Effect of Lattice Impurities on the Thermal Conductivity of β-$Si_3N_4$, *Journal of the European Ceramic Society, 23* (2003), 1, pp. 55-60
[17] Yokota, H., *et al*., Effect of Large β-$Si_3N_4$ Particles on the Thermal Conductivity of β-$Si_3N_4$ Ceramics, *Journal of the European Ceramic Society, 23* (2003), 8, pp. 1175-1182
[18] Hirosaki, N., *et al*., Molecular Dynamics Calculation of the Ideal Thermal Conductivity of Single-Crystal α- and β-$Si_3N_4$, *Phys. Rev. B, 65* (2002), 134110
[19] Duan, Y., *et al*., High Thermal Conductivity Silicon Nitride Ceramics Prepared by Pressureless Sintering with Ternary Sintering Additives, *Int. J. Applied Ceramic Tech., 16* (2019), 4, pp. 1399-1406
[20] Kitayama, M., *et al*., Thermal Conductivity of β-$Si_3N_4$: II, Effect of Lattice Oxygen, *Journal of the American Ceramic Society, 83* (2000), 8, pp. 1985-1992
[21] Watari, K., High Thermal Conductivity Non-Oxide Ceramics., *J. Ceram. Soc. Japan, 109* (2001), 1265, pp. S7-S16
[22] Kitayama, M., *et al*., Oxygen Content in ß-$Si_3N_4$ Crystal Lattice, *Journal of the American Ceramic Society, 82* (1999), 11, pp. 3263-3265

[23] Yang, C., *et al*., Effect of MgF2 Addition on Mechanical Properties and Thermal Conductivity of Silicon Nitride Ceramics, *Ceramics International, 45* (2019), 10, pp. 12757-12763
[24] Dressler, W., Riedel, R., Progress in Silicon-Based Non-Oxide Structural Ceramics, *International Journal of Refractory Metals and Hard Materials, 15* (1997), 1-3, pp. 13-47
[25] Hirosaki, N., *et al*., Thermal Conductivity of Gas-Pressure-Sintered Silicon Nitride, *Journal of the American Ceramic Society, 79* (1996), 11, pp. 2878-2882
[26] Watari, K., *et al*., Temperature Dependence of Thermal Coefficients for HIPped Silicon Nitride, *J. Ceram. Soc. Japan, 97* (1989), 1122, pp. 174-181
[27] Yokota, H., *et al*., Effect of Lattice Defects on the Thermal Conductivity of β-$Si_3N_4$, *Journal of the European Ceramic Society, 23* (2003), 10, pp. 1751-1759
[28] Akimune, Y., *et al*., Raman Spectroscopic Analysis of Structural Defects in Hot Isostatically Pressed Silicon Nitride., *J. Ceram. Soc. Japan, 107* (1999), 1244, pp. 339-342
[29] Hirosaki, N., *et al*., Transmission Electron Microscopy Observation of Second-Phase Particles in β-$Si_3N_4$ Grains, *Journal of Materials Research, 14* (1999), July, pp. 2959-2965
[30] Okamoto, Y., *et al*., Effect of Sintering Additive Composition on the Thermal Conductivity of Silicon Nitride, *J. Mater. Res., 13* (1998), Jan., pp. 3473-3477
[31] Lin, Y., *et al*., Study on the Thermal Conductivity of Silicon Nitride Ceramics with Magnesia and Yttria as Sintering Additives, *Materials Letters, 57* (2002), 1, pp. 15-19
[32] Yeom, H.-J., *et al*., Electrical, Thermal and Mechanical Properties of Silicon Carbide–Silicon Nitride Composites Sintered with Yttria and Scandia, *Journal of the European Ceramic Society, 35* (2015), 1, pp. 77-86
[33] Lu, T., *et al*., Fabrication of High Thermal Conductivity Silicon Nitride Ceramics by Pressureless Sintering with MgO and $Y_2O_3$ as Sintering Additives, *Ceramics International, 46* (2020), 17, pp. 27175-27183
[34] Yokota, H., Ibukiyama, M., Micro-structure Tailoring for High Thermal Conductivity of β-Si3N4 Ceramics, *Journal of the American Ceramic Society, 86* (2003), 1, pp. 197-199
[35] Kitayama, M., *et al*., Thermal Conductivity of Beta-Si(3)N(4): III, Effect of Rare-Earth (RE = La, Nd, Cd, Y, Yb, and Sc) Oxide Additives, *Journal of the American Ceramic Society, 84* (2001), 2, pp. 353-358
[36] Thomas, A., Muller, G., Determination of the Concentration of Oxygen Dissolved in the AlN Lattice by Hot Gas Extraction from AlN Ceramics, *Journal of the European Ceramic Society, 8* (1991), 1, pp. 11-19
[37] Kleebe, H., *et al*., Statistical Analysis of the Intergranular Film Thickness in Silicon Nitride Ceramics, *Journal of the American Ceramic Society, 76* (1993), 8, pp. 1969-1977
[38] Raghavan, V. R., Martin, H., Modelling of Two-Phase Thermal Conductivity, *Chemical Engineering and Processing: Process Intensification, 34* (1995), 5, pp. 439-446
[39] Kitayama, M., *et al*., Thermal Conductivity of ß-$Si_3N_4$: I, Effects of Various Microstructural Factors, *Journal of the American Ceramic Society, 82* (1999), 11, pp. 3105-3112
[40] Hayashi, H., *et al*., MgSiN2 Addition as a Means of Increasing the Thermal Conductivity of β-Silicon Nitride, *Journal of the American Ceramic Society, 84* (2001), 12, pp. 3060-3062
[41] Jackson, T. B., *et al*., High-Thermal-Conductivity Aluminum Nitride Ceramics: The Effect of Thermodynamic, Kinetic, and Microstructural Factors, *J. of the Ame. Ce. Soc., 80* (1997), 6, pp. 1421-1435
[42] Zhu, X., *et al*., Processing and Thermal Conductivity of Sintered Reaction-Bonded Silicon Nitride: (II) Effects of Magnesium Compound and Yttria Additives, *J. of the Ame. Ce. Soc., 90* (2007), 6, pp. 1684-1692
[43] Zhu, X. W., *et al*., A Strategy for Fabricating Textured Silicon Nitride with Enhanced Thermal Conductivity, *Journal of the European Ceramic Society, 34* (2014), 10, pp. 2585-2589
[44] Zhou, Y., *et al*., A Tough Silicon Nitride Ceramic with High Thermal Conductivity, *Advanced Materials, 23* (2011), 39, pp. 4563-4567
[45] Kong, J. H., *et al*., Self-Reinforced and High-Thermal Conductivity Silicon Nitride by Tailoring α-β Phase Ratio with Pressureless Multi-Step Sintering, *Ceramics International, 47* (2021), 9, pp. 13057-13064
[46] Watari, K., *et al*., Effect of Grain Size on the Thermal Conductivity of $Si_3N_4$, *Journal of the American Ceramic Society, 82* (1999), 3, pp. 777-779
[47] Zhou, Y., X. *et al*., Sintered Reaction-Bonded Silicon Nitride with High Thermal Conductivity and High Strength, *Int. J. Applied Ceramic Tech., 5* (2008), 2, pp. 119-126
[48] Vučković, A., *et al*., Effect of β-Si3N4 Seeds on Densification and Fracture Toughness of Silicon Nitride, *Ceramics International, 32* (2006), 3, pp. 303-307
[49] Zhou, Y., *et al*., Fracture Resistance Behavior of High-Thermal-Conductivity Silicon Nitride Ceramics, *Int. J. Applied Ceramic Tech., 11* (2014), 5, pp. 872-882

[50] Moulson, A. J., Reaction-Bonded Silicon Nitride: Its Formation and Properties, *Journal of Materials Science, 14* (1979), May, pp. 1017-1051

[51] Haggerty, J., Lightfoot, A., Opportunities for Enhancing the Thermal Conductivity of SiC and Si3N4 Ceramics Through Improved Processing, in: *Ceramic Engineering and Science Proceedings*, *16* (2008), 4, pp. 475-487

[52] Zhu, X., *et al*., Effect of Sintering Additive Composition on the Processing and Thermal Conductivity of Sintered Reaction-Bonded $Si_3N_4$, *Journal of the American Ceramic Society, 87* (2004), 7, pp. 1398-1400

[53] Zhu, Z., *et al*., Processing and Thermal Conductivity of Sintered Reaction-Bonded Silicon Nitride. I: Effect of Si Powder Characteristics, *Journal of the American Ceramic Society, 89* (2006), 11, pp. 3331-3339

[54] Hirao, K., *et al*., High Thermal Conductivity Silicon Nitride Ceramics, *Journal of the Korean Ceramic Society, 49* (2012), 4, pp. 380-384

[55] Zhou, Y., *et al*., Development of High-Thermal-Conductivity Silicon Nitride Ceramics, *Journal of Asian Ceramic Societies, 3* (2015), 3, pp. 221-229

[56] Sillapasa, K., *et al*., Effects of Silicon Powder Size on the Processing of Reaction-Bonded Silicon Nitride, *J. Met. Mater. Miner., 15* (2005), 2, pp. 97-102

[57] Nikonam-Mofrad, R., *et al*., A Comparative Study on Nitridation Mechanism and Microstructural Development of Porous Reaction Bonded Silicon Nitride in the Presence of CaO, MgO and $Al_2O_3$, *Journal of Asian Ceramic Societies, 8* (2020), 3, pp. 873-890

[58] Zhu, X., Sakka, Y., Textured Silicon Nitride: Processing and Anisotropic Properties, *Science and Technology of Advanced Materials, 9* (2008), 033001

[59] Li, B., *et al*., Measuring the Anisotropic Thermal Diffusivity of Silicon Nitride Grains by Thermoreflectance Microscopy, *Journal of the European Ceramic Society, 19* (1999), 8, pp. 1631-1639

[60] Hirao, K., *et al*., High Thermal Conductivity in Silicon Nitride with Anisotropie Micro-structure, *Journal of the American Ceramic Society, 79* (1996), 9, pp. 2485-2488

[61] Hirao, K., *et al*., Micro-structure Control of Silicon Nitride by Seeding with Rodlike β-Silicon Nitride Particles, *Journal of the American Ceramic Society, 77* (1994), 7, pp. 1857-1862

[62] Hirao, K., *et al*., Processing Strategy for Producing Highly Anisotropic Silicon Nitride, *Journal of the American Ceramic Society, 78* (1995), 6, pp. 1687-1690

[63] Watari, K., *et al*., Hot Isostatic Pressing to Increase Thermal Conductivity of $Si_3N_4$ Ceramics, *J. Mater. Res., 14* (1999), Apr., pp. 1538-1541

[64] Sakka, Y., Suzuki, T. S., Textured Development of Feeble Magnetic Ceramics by Colloidal Processing Under High Magnetic Field, *J. Ceram. Soc. Japan, 113* (2005), 1313, pp. 26-36

[65] Sakka, Y., *et al*., Fabrication and Some Properties of Textured Alumina-Related Compounds by Colloidal Processing in High-Magnetic Field and Sintering, *J. of the Eu. Ceramic Society, 28* (2008), 5, pp. 935-942

[66] Zhu, X. W., *et al*., The c-Axis Texturing of Ceeded $Si_3N_4$ with β-$Si_3N_4$ Whiskers by Slip Casting in a Rotating Magnetic Field, *Acta Materialia, 58* (2010), 1, pp. 146-161

Paper submitted: June 15, 2024
Paper revised: August 21, 2024
Paper accepted: August 23, 2024